Skeletal Radiol (2003) 32:687–694
DOI 10.1007/s00256-003-0668-3

ARTICLE

Mark S. Collins
Takashi Koyama
Ronald G. Swee
Carrie Y. Inwards

Clear cell chondrosarcoma: radiographic, computed tomographic, and magnetic resonance findings in 34 patients with pathologic correlation

Received: 29 July 2002
Revised: 23 May 2003
Accepted: 27 May 2003
Published online: 7 October 2003

Abstract *Objective:* To describe the radiographic features of clear cell chondrosarcoma (CCCS), including the computed tomographic (CT) and magnetic resonance (MR) findings, and to correlate them with the histopathologic findings. *Design and patients:* A retrospective review was carried out of 72 patients with histopathologically confirmed CCCS. Imaging studies were available for 34 patients: conventional radiographs (*n*=28), CT scans (*n*=14), and MR images (*n*=15). Radiographic studies were reviewed by three radiologists who rendered a consensus opinion; the studies were correlated with the histopathologic findings. *Results:* Of the 34 patients with imaging studies, 30 were male and 4 were female (mean age 38.6 years; range 11–74 years). Twenty-two lesions were in long bones (15, proximal femur; 1, distal femur; 1, proximal tibia; 5, proximal humerus) and 11 were in flat bones (5, vertebra; 4, rib; 1, scapula; 1, innominate). One lesion occurred in the tarsal navicular bone. Typically, long bone lesions were located in the epimetaphysis (19/22) and were lucent with a well-defined sclerotic margin and no cortical destruction or periosteal new bone formation. More than one-third of the long bone lesions contained matrix mineralization with a characteristic chondroid appearance. Pathologic fractures were present in six long bone lesions (4, humerus; 2, femur). Lesions in the proximal humerus were more likely to have indistinct margins (4/5) and extend into the diaphysis. Flat bone lesions were typically lytic and expansile and occasionally demonstrated areas of cortical disruption. Typically, matrix mineralization, when present, was amorphous. MR imaging, when available, was superior to conventional radiographs for demonstrating the intramedullary extent of a lesion as well as soft tissue extension. CT images better delineated the presence of cortical destruction and the character of matrix mineralization patterns. CCCS lesions were typically low signal intensity on T1-weighted images and moderately or significantly bright on T2-weighted images. Areas of lesion heterogeneity on T1- and T2-weighted images and on post-gadolinium T1-weighted images corresponded pathologically to areas of mineralization, intralesional hemorrhage, and cystic changes. Adjacent bone marrow edema was typically absent (12/15) or only minimally observed in a few cases (3/15). No cases examined with MR imaging demonstrated periosteal new bone formation. *Conclusions:* CCCS typically presents radiographically as a geographic lytic lesion located in the epimetaphyseal region of long bones. Most commonly lesions are found in the proximal femur, followed by the proximal humerus. Lesions within the proximal humerus may exhibit more aggressive features. Lesions in the axial skeleton are typically expansile and destructive, often with soft tissue extension and lack of mineralization. MR imaging may show the presence or absence of bone marrow edema.

Keywords Clear cell chondrosarcoma · Computed tomography · Histopathology · Radiography · Magnetic resonance · Retrospective study

M. S. Collins (✉) · T. Koyama
R. G. Swee · C. Y. Inwards
Department of Radiology,
Mayo Clinic,
200 First Street SW, Rochester, MN 55905, USA
e-mail: collins.mark@mayo.edu

Introduction

Clear cell chondrosarcoma (CCCS) is a distinct variant of chondrosarcoma of low-grade malignancy that was first described in 1976 by Unni et al. [1]. Histologically it is characterized by tumor cells with abundant clear cytoplasm arranged in a lobulated growth pattern. Unlike conventional chondrosarcoma, CCCS has a strong tendency to arise in the epiphyses of long tubular bones, especially the proximal femur. Radiographically, CCCS frequently resembles the more common benign chondroblastoma or giant cell tumor. Although CCCS is slowly progressive, distant metastases have been reported [1, 2, 3, 4]. Rarely, CCCS may undergo dedifferentiation, resulting in a poor clinical prognosis [5]. Because recurrence is frequent when CCCS is treated conservatively with simple excision and curettage, more aggressive treatment such as en bloc resection is required [2]. For this reason, it is important to make a radiographic distinction between CCCS and benign epiphyseal lesions, such as chondroblastoma or giant cell tumor. Conventional radiographic findings of CCCS have been previously described [1, 2, 6]. However, the value of computed tomography (CT) and magnetic resonance (MR) features in the imaging diagnosis of CCCS has not been fully discussed. Our series is the largest that includes CT and MR images. The purpose of our study was to describe the imaging features of CCCS, including CT and MR findings, and to correlate them with the histopathologic findings.

Patients and methods

A review of our institution's pathologic records and consultation files from 1990 to 2000 identified 74 patients with pathologically confirmed CCCS. Two cases of dedifferentiated CCCS were excluded. Imaging studies were available for 34 patients in our study. These 34 patients (30 males, 4 females; mean age 38.6 years, range 11–74 years) constituted our study population.

The available imaging studies included conventional radiographs for 28 patients, CT images for 14 patients, and MR images for 15 patients. Because the MR images were performed at several institutions, techniques varied considerably. All studies included conventional spin-echo T1-weighted images (n=15). Various T2-weighted image sequences were used, including conventional spin-echo (n=4), fast spin-echo (n=6), and gradient-recalled echo (n=2). In three cases, inversion recovery sequences were used in place of T2 sequences (short tau inversion recovery=1; fast-spin echo inversion recovery=2). Contrast-enhanced T1-weighted images were available for seven patients.

The radiographic images were retrospectively reviewed by three radiologists who collectively rendered a consensus interpretation. The imaging features of the tumor that were evaluated included location, growth pattern and character, margination, presence of a sclerotic rim, bony expansion, periosteal new bone formation, cortical thinning, cortical destruction, presence and character of mineralization, pathologic fracture, and soft tissue extension. MR images were reviewed for T1 and T2 signal characteristics of the lesions. In addition, lesion homogeneity or heterogeneity and post-enhancement patterns were evaluated. The intramedullary extent of the lesion, the presence of soft tissue extension, and the presence or absence of adjacent bone marrow edema were also assessed. The location of the lesion was arbitrarily designated as epiphyseal, metaphyseal or diaphyseal relative to the open physis in skeletally immature patients and the physeal scar in skeletally mature patients. Lesions which involved both the epiphysis and metaphysis were described as being "epimetaphyseal" in location.

Hematoxylin and eosin-stained microscopic sections from each of the 34 tumors were reviewed. The histologic features evaluated included amount of bone production, presence or absence of hyaline cartilage, cystic change (i.e., aneurysmal bone cyst-like features), and hemorrhage. The microscopic slides were reviewed without knowledge of the location and imaging findings of each lesion. The date of the radiographic images and pathologic specimens was compared for each lesion.

Results

Radiography

Conventional radiographs were available in 28 of the 34 patients with imaging studies. Twenty-two lesions were located in long bones, including the proximal femur (n=15), proximal humerus (n=5), distal femur (n=1), and proximal tibia (n=1). Other locations included vertebra (n=5), rib (n=4), scapula (n=1), posterior iliac wing (n=1), and tarsal navicular bone (n=1). Among the four cases occurring in ribs, three lesions were located adjacent to the costochondral junction, and one lesion occurred in the proximal end near the costovertebral joint. Among the five vertebral lesions, three occurred in the posterior elements of the thoracic spine and two occurred in the body of the lumbar and cervical spine. One of these two lesions also extended into the posterior elements.

Conventional radiographs were available for all 22 cases involving the long bones. All lesions presented as a geographic osteolytic area. The lesions were located in the epiphysis (n=3) or epimetaphysis (n=19) (Fig. 1A). Four humeral lesions demonstrated bone expansion and diaphyseal extension (Fig. 2A). Two of these four lesions showed poor margination with permeative lucency at the distal extent. Nine femoral lesions demonstrated well-defined margins entirely. Nine lesions located in the proximal femur (n=6) and proximal humerus (n = 3) (Fig. 3A) displayed indistinct distal margins. Thirteen lesions were accompanied by a sclerotic rim (Fig. 1A). Pathologic fracture was seen in four humeral lesions (Fig. 2) and two femoral lesions. One of these two was associated with segmental collapse of the articular surface, closely resembling avascular necrosis.

Among the cases not involving long bones, one lesion in the tarsal navicular bone showed a geographic osteolytic pattern with a well-defined margin. Lesions located within the vertebrae, ribs, and scapula were typically lytic and expansile with poorly defined margins.

Fig. 1A–E Clear cell chondrosarcoma in the proximal femur of a 47-year-old male patient. **A** Anteroposterior radiograph demonstrates a well-marginated osteolytic lesion in the epimetaphysis of the right hip. **B** Axial T1-weighted magnetic resonance (MR) image shows a well-defined lesion with low signal intensity. **C** Axial T2-weighted MR image demonstrates increased signal intensity within the lesion with focal areas of brighter internal signal intensity (*arrow*) which correspond to internal cystic areas. **D** Coronal post-contrast T1-weighted MR image shows diffuse lesion enhancement other than the areas of focal cystic change (*arrow*). **E** Gross pathologic specimen demonstrates focal areas of secondary aneurysmal bone cyst formation, which correspond to the cystic areas seen on MR images

In all cases, periosteal new bone formation was absent. Mineralization was seen in 13 lesions. In eight cases, the character of the mineralization was punctate, with a typical chondroid appearance (Fig. 4A). In five cases, mineralization was more amorphous and not obviously chondroid in nature (Fig. 2A).

CT findings

In 10 cases, both conventional radiographs and CT images were available. Matrix mineralization was demonstrated in six of the cases, in four of which the character of the mineral was better displayed on CT images than on conventional radiographs (Fig. 4). Tumor extension into the soft tissue was clearly recognized on CT in two vertebral lesions (Fig. 5) and one scapular lesion (Fig. 6B). Only CT images were available for two rib lesions, which appeared as well-marginated, expansile lytic lesions.

MR findings

Fifteen of the study cases included MR images. On T1-weighted sequences, the lesions were low signal intensity in the majority of cases (n=13) (Fig. 1B). Two lesions contained focal central areas of bright T1 signal in-

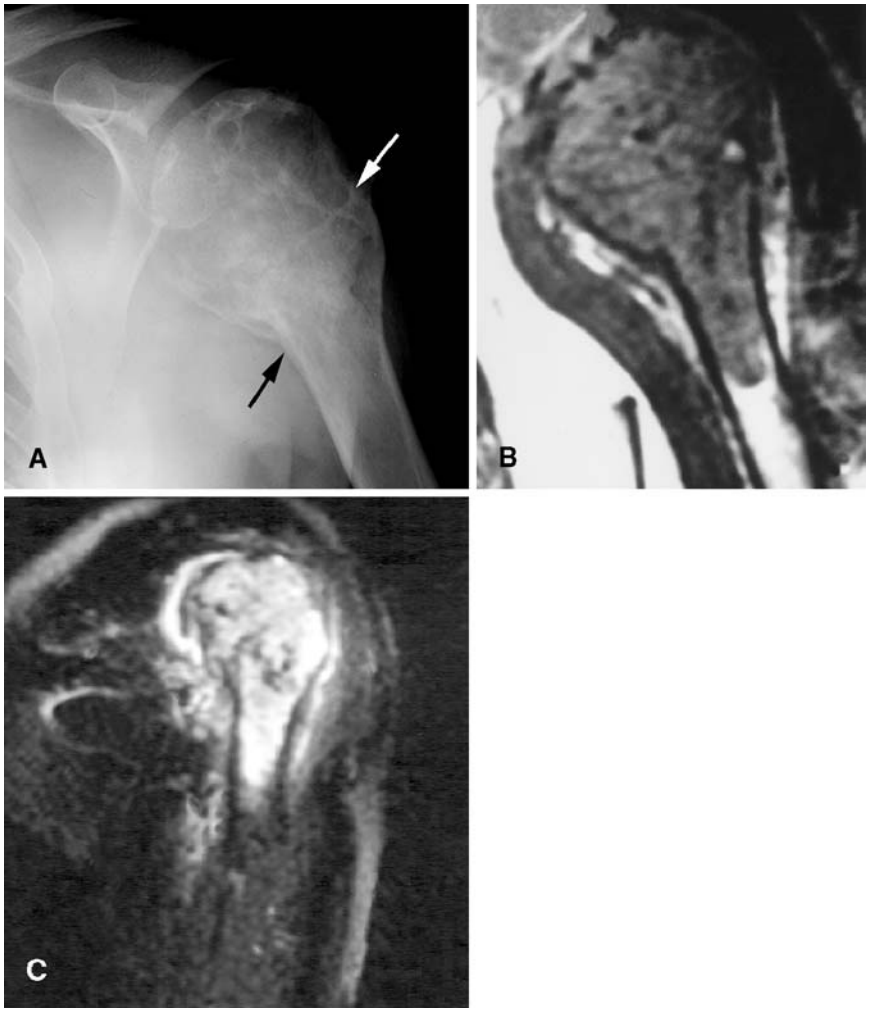

Fig. 2A–C Clear cell chondrosarcoma in the proximal humerus of a 37-year-old female patient. **A** Anteroposterior radiograph demonstrates an expansile osteolytic lesion with a geographic pattern. The distal margin is indistinct, and there is an associated pathologic fracture (*arrows*). Amorphous matrix mineralization is present. **B** Coronal T1-weighted magnetic resonance (MR) image more clearly demonstrates the intramedullary extent of the lesion, which extends to the proximal diaphysis. Scattered, punctate areas of decreased signal intensity are consistent with mineralization. **C** Coronal T2-weighted MR image demonstrates heterogeneous bright intralesional signal. There are some areas of increase T2 signal in the overlying soft tissues consistent with perifractural hemorrhage and edema

tensity due to intralesional hemorrhage. Typically, lesion heterogeneity was due to scattered areas of decreased T1 signal intensity corresponding to matrix mineralization seen on conventional radiographs. On T2-weighted and short tau inversion recovery images, lesions were high signal intensity. Two lesions were homogeneously bright. The remaining lesions were heterogeneously bright on the T2-weighted images. Focal areas of brighter T2 signal often occurred in intralesional cystic areas (*n*=7) (Fig. 1C), some of which had a multilocular appearance (*n*=2) or fluid-fluid levels (*n*=2). Scattered areas of decreased T1 and T2 signal intensity correlated with matrix mineralization (*n*=4) (Figs. 2B, 3B). Increased T2 signal intensity of adjacent bone marrow was minimally observed in three cases. One case demonstrated increased T2 signal in the adjacent soft tissues due to perifractural hemorrhage and edema (Fig. 2C). Otherwise, the adjacent soft tissues were normal in appearance. Postcontrast T1-weighted images, available for seven cases, showed either a diffuse (*n*=1) or heterogeneous (*n*=6) pattern of enhancement. The heterogeneous appearance was due to the presence of unenhanced areas (Fig. 3C) that corresponded to areas of either mineralization (*n*=2) (Fig. 3C) or cystic change (*n*=4) (Fig. 1C).

In 12 cases with both MR images and conventional radiographs available, MR more clearly delineated the intramedullary extent of the lesion, including seven cases that had indistinct margins on the conventional radiographs (Fig. 2B). Only MR images were available for three cases, occurring in vertebrae (*n*=2) and an iliac wing (*n*=1). In both vertebral lesions, soft tissue extension was demonstrated on MR images.

Histologic findings

The diagnosis of clear cell chondrosarcoma was confirmed in all 34 cases. All lesions were characterized by the presence of clear cells with characteristic round nuclei. In 22 lesions occurring in long bones, bone formation was abundant (*n*=17) or moderate (*n*=2). Hyaline

Fig. 3A–C Clear cell chondrosarcoma in the proximal humerus of a 28-year-old male patient. **A** Anteroposterior radiograph shows a well-marginated osteolytic epiphyseal lesion with typical chondroid type mineralization. **B** Coronal T2-weighted MR image demonstrates heterogeneously bright signal intensity throughout the lesion with focal areas of decreased signal intensity corresponding to matrix mineralization (*arrow*). **C** Coronal post-gadolinium T1-weighted MR image shows heterogeneous lesion enhancement with scattered unenhanced foci also corresponding to areas of punctate mineralization (*arrow*)

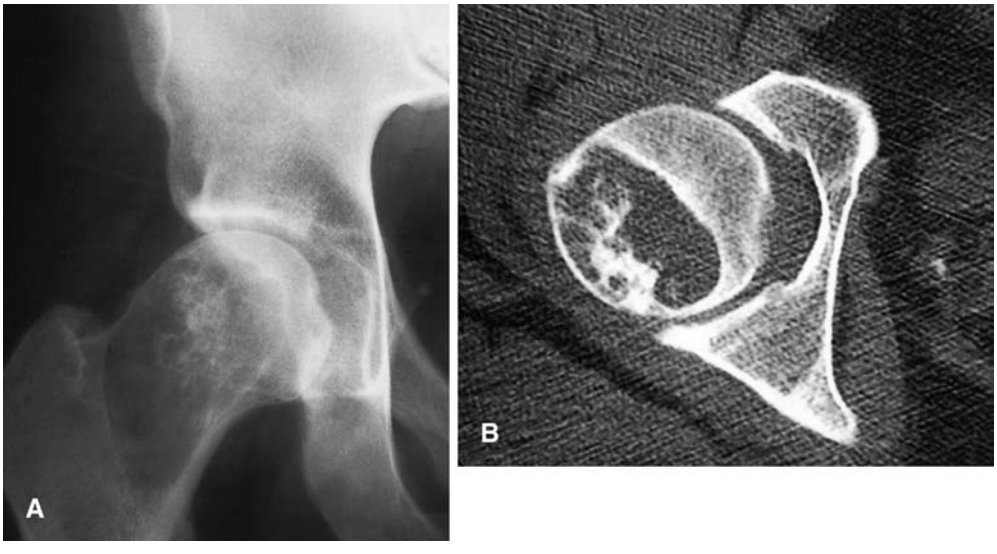

Fig. 4A, B Clear cell chondrosarcoma in the proximal femur of a 31-year-old male patient. **A** Anteroposterior radiograph of the right hip demonstrates a partially well-defined osteolytic lesion with punctate mineralization with typical chondroid appearance. **B** Axial CT images more clearly demonstrate the chondroid character of mineralization and the intramedullary extent of the lesion

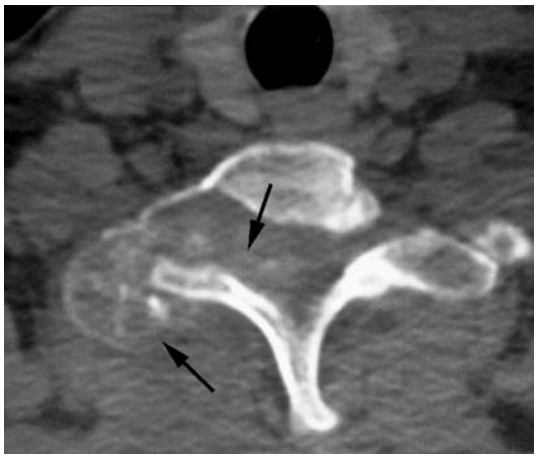

Fig. 5 Clear cell chondrosarcoma in the first thoracic vertebra of a 35-year-old male patient. Axial CT images demonstrate a lytic expansile mass arising from the posterior elements. There is cortical destruction with soft tissue extension (*arrows*). The mass is partially mineralized. Osteoblastoma could also have this appearance

cartilage was abundant (*n*=13), moderate (*n*=3), or absent or minimal (*n*=6). In the five vertebral lesions and the single iliac lesion, bone formation and a cartilaginous component were absent or minimal. The remaining tumors occurring in other sites contained abundant bone formation and cartilage. Cystic changes due to secondary aneurysmal bone cyst formation were seen in four lesions. Three lesions contained prominent areas of intralesional hemorrhage.

Comparison of imaging and histologic findings

In all 13 lesions with radiographically apparent mineral, the presence of abundant osteoid and woven bone formation was microscopically confirmed. Histologic evidence of an abundant cartilaginous component was confirmed in eight lesions with typical chondroid mineralization seen on conventional radiographs. However, eight lesions without radiographically discernible mineralization contained abundant bone formation. In three lesions with bright MR T2 signal intensity with microcystic appearance and five lesions with focal areas of bright intensity on T2-weighted images, focal aneurysmal bone cyst changes (*n*=5) or prominent areas of hemorrhage (*n*=3) were histologically identified. In three other lesions with heterogeneous high signal intensity on T2-weighted MR images, chondroid matrix was abundant histologically. In one lesion with slightly increased signal intensity on T2-weighted images, the amount of hyaline cartilage was less prominent.

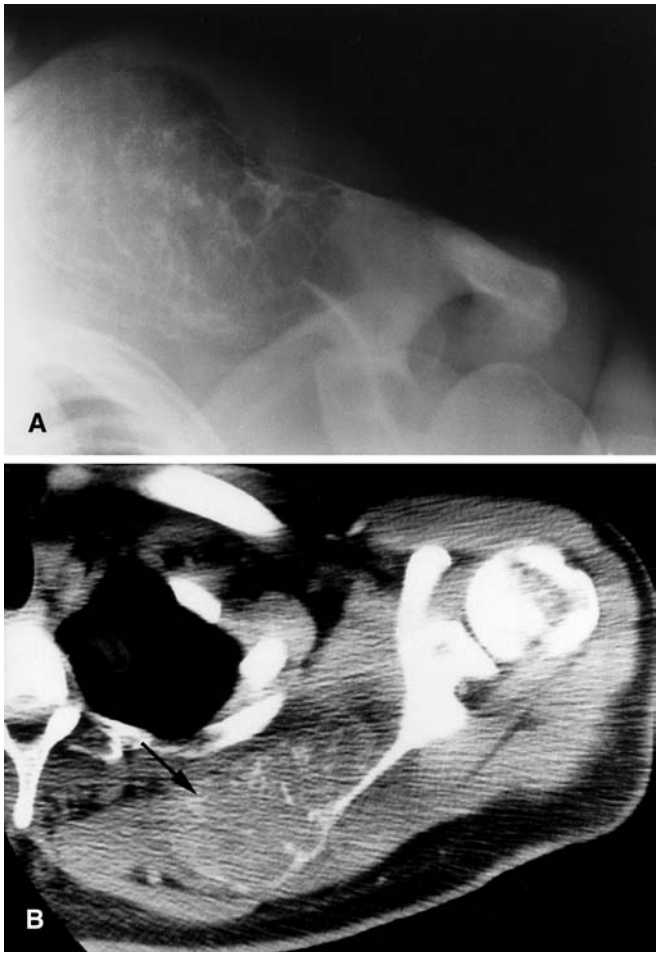

Fig. 6A, B Clear cell chondrosarcoma in the left scapula of a 26-year-old male patient. **A** Anteroposterior radiograph demonstrates a partially mineralized, poorly defined, expansile, lytic mass arising from the upper scapula. **B** Axial CT images better define the lesion and demonstrate some cortical disruption with soft tissue extension (*arrow*)

Discussion

CCCS is a low-grade malignancy, accounting for approximately 2% of all chondrosarcomas. Unlike conventional chondrosarcoma, CCCS commonly involves the epiphysis and epimetaphysis of long bones. The proximal femur is the most frequent site of involvement (68%), followed by the proximal humerus (23%). Although CCCS occurs in patients of various ages, it usually occurs in the third, fourth, or fifth decade [2]. The age distribution in our series is in agreement with previous reports. The peak age of occurrence is older than that for patients with chondroblastoma. Unlike other cartilage tumors, CCCS has shown a definite male predilection (34/47) [2]. This predilection was even more prominent in our series (29/34).

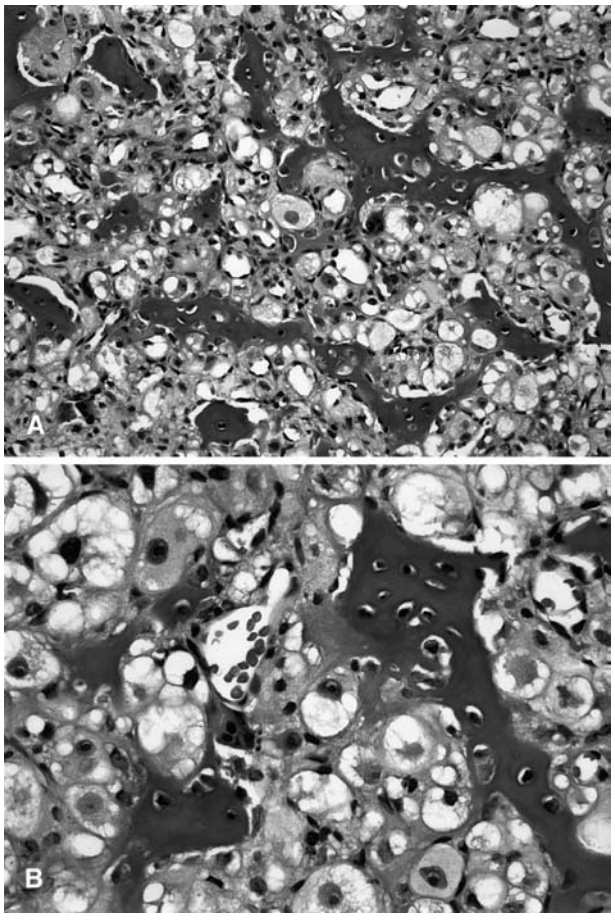

Fig. 7 **A** Irregular trabeculae of woven bone scattered throughout sheets of tumor cells in this clear cell chondrosarcoma involving the proximal humerus. **B** Higher magnification shows cells with abundant clear or faintly granular cytoplasm and central round nuclei containing prominent nucleoli

Microscopically, CCCS is characterized by the presence of cells with clear or granular cytoplasm and a lobulated architecture [1]. Nuclei are round and located centrally within the lucent cytoplasm (Fig. 7A, B). CCCS contains variable amounts of hyaline cartilage, osteoid production, and focal cystic changes such as aneurysmal bone cyst formation, which makes the histologic features of CCCS rather heterogeneous. About 50% of the tumors contain nodules of conventional chondrosarcoma (Fig. 8) [1, 2].

Radiographically, the majority of lesions in long bones are located in the epimetaphysis. Rarely, diaphyseal extension is seen. On conventional radiographs, CCCS typically appears as a well-marginated radiolucent area with distinct sclerotic borders. However, indistinct margins may be seen distally. Lesions in the proximal humerus in our series appeared to be more aggressive than other long bone lesions. Frequently, the humeral lesions exhibited diaphyseal extension, bone expansion, indistinct margination, and pathologic fracture. Mineralization was seen in about one-third of our cases. Unlike findings in previous reports, in our series, typical chondroid mineral was commonly seen [2, 6]. Soft tissue extension is unusual in lesions located in long bones.

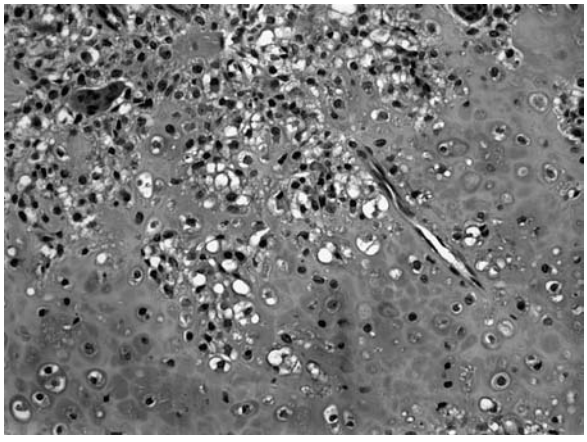

Fig. 8 Clear cell chondrosarcoma containing an area of conventional chondrosarcoma and a few multinucleated giant cells

Although CT findings did not differ significantly from those demonstrated on conventional radiographs, CT was more effective in detecting and characterizing the pattern of mineralization and cortical destruction. Recognition of chondroid mineralization is important in making the correct diagnosis. Lesions occurring in flat bones or vertebrae are commonly associated with cortical destruction and soft tissue extension [2, 7]. In these cases, CT is superior to conventional radiographs in displaying these findings.

MR imaging was also helpful in demonstrating the intramedullary extent of the lesion, its internal architecture, soft tissue extension, and signal changes in surrounding bone marrow. Signal characteristics of CCCS on MR images have not been fully discussed. Cohen et al. [8] reported a case of CCCS that demonstrated slightly increased T2 signal intensity, stressing that the signal intensity was less than that of conventional chondrosarcoma. Fobben et al. [9] reported a case of CCCS with high signal intensity on long TR and short TE images. In our series, the majority of cases showed heterogeneous bright signal intensity on T2-weighted images. One of the reasons for the heterogeneous appearances was mineralization, which exhibited distinctly low signal intensity on all MR sequences. Focal areas of brighter signal intensity on T2-weighted images corresponded pathologically to hyaline cartilage, focal cystic changes, or hemorrhage.

When CCCS occurs in long bones, the more common benign lesions involving the epiphysis, such as giant cell tumor or chondroblastoma, are the main diagnostic considerations. Chondroblastoma usually occurs in younger

patients and is located completely within the epiphysis with distinct sclerotic margins. CCCS lesions occur in older patients and are typically larger than chondroblastoma and involve the epiphysis and metaphysis with occasional diaphyseal extension. The aggressive features in the humeral lesions of CCCS demonstrated in our series, including bone expansion, poor margination, and diaphyseal extension, are unusual in cases of chondroblastoma. However, in some cases, distinguishing between CCCS and chondroblastoma on conventional radiographs can be difficult. On MR T2-weighted images, giant cell tumor and chondroblastoma usually exhibit low to intermediate signal intensity [10, 11, 12]. These findings could be useful in distinguishing chondroblastoma from CCCS. However, chondroblastoma and giant cell tumor can exhibit heterogeneous bright signal intensity on T2-weighted images, because of the presence of focal cystic changes, similar to CCCS. For this reason, a specific diagnosis of CCCS based solely on MR signal characteristics can be difficult, as is often the case with most primary bone tumors.. Prominent bone marrow edema, often seen with chondroblastoma, is rarely seen with CCCS; when present, it is minimal. Occasionally, lesions in the proximal femur can simulate avascular necrosis. However, avascular necrosis often exhibits distinct MR features, such as a dark linear margin on T1-weighted images and a "double line sign" on T2-weighted sequences [13].

Radiographic diagnostic considerations in lesions occurring in sites other than the long bones include osteoblastoma, aneurysmal bone cyst, fibrous dysplasia, conventional chondrosarcoma, metastases, and myeloma. Because both CCCS and conventional chondrosarcoma may contain matrix mineralization, distinguishing between them may be difficult. However, the distinction has little clinical significance because treatment is not significantly altered. If matrix mineralization is not present, radiographic findings may not allow a specific diagnosis of CCCS.

In conclusion, CCCS typically appears as a geographic osteolytic lesion located within the epiphyseal-metaphyseal region of long bones, usually in the third decade of life and beyond. CCCS is most frequently located in the proximal femur, followed by the proximal humerus. Lesions in the proximal humerus may exhibit more aggressive features than lesions in other long bones. This feature has not been previously noted. More than one-third of long bone lesions contain matrix mineralization that is usually typical chondroid. Lesions in the vertebrae or flat bones appear destructive or expansile, and they typically exhibit soft tissue extension and lack radiographic evidence of matrix mineralization. CT and MR imaging are superior to conventional radiographs in demonstrating the intramedullary extent of the lesion, cortex disruption, and soft tissue extension. CT is superior for demonstrating not only these findings but also the character of mineralization. MR images typically demonstrate heterogeneous internal architecture, reflecting pathologic characteristics, with the presence or absence of surrounding bone marrow edema. The age of the patient, the lack of bone marrow edema, and the imaging characteristics described ought to permit separation of the relatively rare CCCS from the more common chondroblastoma.

References

1. Unni KK, Dahlin DC, Beabout JW, Sim FH. Chondrosarcoma: clear-cell variant. A report of sixteen cases. J Bone Joint Surg Am 1976; 58:676–683.
2. Bjornsson J, Unni KK, Dahlin DC, Beabout JW, Sim FH. Clear cell chondrosarcoma of bone: observations in 47 cases. Am J Surg Pathol 1984; 8:223–230.
3. Kumar R, David R, Cierney G III. Clear cell chondrosarcoma. Radiology 1985; 154:45–48.
4. Le Charpentier Y, Forest M, Postel M, Tomeno B, Abelanet R. Clear-cell chondrosarcoma: a report of five cases including ultrastructural study. Cancer 1979; 44:622–629.
5. Kalil RK, Inwards CY, Unni KK, et al. Dedifferentiated clear cell chondrosarcoma. Am J Surg Pathol 2000; 24:1079–1086.
6. Present DA, Bonar SF, Greenspan A, Paonessa K. Clear-cell chondrosarcoma: an unusual case complicated by a microinfiltrative pattern of bone marrow involvement and postsurgical myositis ossificans. Clin Orthop 1988; 237:164–169.
7. Bagley L, Kneeland JB, Dalinka MK, Bullough P, Brooks J. Unusual behavior of clear cell chondrosarcoma. Skeletal Radiol 1993; 22:279–282.
8. Cohen EK, Kressel HY, Frank TS, et al. Hyaline cartilage-origin bone and soft-tissue neoplasms: MR appearance and histologic correlation. Radiology 1988; 167:477–481.
9. Fobben ES, Dalinka MK, Schiebler ML, et al. The magnetic resonance imaging appearance at 1.5 tesla of cartilaginous tumors involving the epiphysis. Skeletal Radiol 1987; 16:647–651.
10. Weatherall PT, Maale GE, Mendelsohn DB, Sherry CS, Erdman WE, Pascoe HR. Chondroblastoma: classic and confusing appearance at MR imaging. Radiology 1994; 190:467–474.
11. Jee WH, Park YK, McCauley TR, et al. Chondroblastoma: MR characteristics with pathologic correlation. J Comput Assist Tomogr 1999; 23:721–726.
12. Yamamura S, Sato K, Sugiura H, Iwata H. Inflammatory reaction in chondroblastoma. Skeletal Radiol 1996; 25:371–376.
13. Sakamoto M, Shimizu K, Iida S, Akita T, Moriya H, Nawata Y. Osteonecrosis of the femoral head: a prospective study with MRI. J Bone Joint Surg Br 1997; 79:213–219.